GULF GENERAL ATOMIC

Gulf-GA-A10803

GAS-COOLED FAST BREEDER REACTOR

QUARTERLY PROGRESS REPORT

FOR THE PERIOD MAY 1, 1971 THROUGH JULY 31, 1971

by

Project Staff

Prepared for the
U.S. Atomic Energy Commission
San Francisco Operations Office
under
Contract AT(04-3)-167
Project Agreement No. 23

Gulf General Atomic Project 393

August 31, 1971

GULF GENERAL ATOMIC COMPANY
P.O. BOX 608, SAN DIEGO, CALIFORNIA 92112

PROGRESS REPORT SERIES

GA-5537	November 1, 1963 to July 31, 1964
GA-6667	August 1, 1964 to July 31, 1965
GA-7645	August 1, 1965 to July 31, 1966
GA-8107	August 1, 1966 to July 31, 1967
GA-8787	August 1, 1967 to July 31, 1968
GA-8895	August 1, 1968 through October 31, 1968
GA-9229	November 1, 1968 through January 31, 1969
GA-9359	February 1, 1969 through April 30, 1969
GA-9639	May 1, 1969 through July 31, 1969
GA-9811	August 1, 1969 through October 31, 1969
GA-9838	November 1, 1969 through January 31, 1970
GA-10517	February 1, 1970 through January 31, 1971
GA-10645	February 1, 1971 through April 30, 1971

ABSTRACT

The tasks of the AEC-supported Gas-Cooled Fast Breeder Reactor (GCFR) program are program planning, core development, fuels and materials development, irradiation tests, and nuclear analysis and reactor physics. The status of the three volumes of the development program plan document for the GCFR demonstration plant is reported. Surveillance of materials included some recent information on cladding materials, which is summarized. The current irradiation test results and analyses are reported for capsule GB-9, which is operating very saticfactorily in ORR and has reached 43,000 MWd/Te. Plans for the irradiation of a similar but improved capsule (GB-10) are discussed. The status of the fast-flux experiment F-1 (X094) in EBR-II and of the five F-1 replacement rods is reported. Results of out-of-pile experiments to develop cladding temperature-monitoring techniques are discussed. Finally, the background and objectives of the GCFR critical assembly program are presented.

CONTENTS

Figures

Tables

1. INTRODUCTION

Gulf General Atomic (GGA) is in its eighth year of U.S. Atomic Energy Commission (AEC) sponsored work on the Gas-Cooled Fast Breeder Reactor (GCFR). The current program effort under AEC sponsorship consists of Task 1000 — Program planning, Task 4100 — Core Development, Task 4200/4400 — Fuels and Material Development, and Task 4700 — Nuclear Analysis and Reactor Physics. The broad objectives of these four tasks and the current efforts on each task during the period covered by this report are summarized below. The work done on each task is presented in Sections 2 through 5. Publications issued during this reporting period are listed in the Appendix.

Gulf General Atomic is also engaged in the privately sponsored GCFR Utility Program that is centered on the development program for a 300-MW(e) GCFR demonstration plant. This and the AEC sponsored work are complementary to each other.

1.1. TASK 1000 — PROGRAM PLANNING

Work on this task is directed toward detailing plans for the technical development of the GCFR concept. The development program planning document will identify and define the developmental items necessary for the design and construction of a 300-MW(e) GCFR demonstration plant, a developmental test program, estimated program costs, and schedule for the development tasks.

1.2. TASK 4100 — CORE DEVELOPMENT

The objective of this task is the engineering development of the reactor core and associated components, including the core support structure and the fuel pressure equalization system.

During this reporting period, studies were made of the interactions between the grid plate and the pressure equalization system and of the vent line connections to the fuel elements. In addition, an economic comparison was made of different rod roughening dimensions.

1.3. TASK 4200/4400 — FUELS AND MATERIALS DEVELOPMENT

GCFR fuel is based on LMFBR fuel development and technology, and therefore, the surveillance of LMFBR fuel and materials irradiation programs is necessary to made available the base technology for the GCFR. Of particular importance is the LMFBR work on fast flux irradiation-induced metal swelling. Some of the pertinent results of experimental work by various investigators on irradiation-induced void formation in metals is summarized in Section 4.1.

The current test results on the irradiation testing of capsule GB-9 in ORR are reported in Section 4.2. The fuel rod continued to operate satisfactorily at 16 kW/ft and maximum cladding temperature of 700°C and reached a burnup of 43,000 MWd/Te. The burnup goal was extended to 75,000 MWd/Te to obtain fission-gas release measurements at higher fuel burnup. The design and analysis of capsule GB-10, a vented capsule similar to but more versatile than GB-9, is about 50% complete.

In the fast-flux irradiation of the F-1 (X094) subassembly in EBR-II, the main objective is to study the behavior of fuel rods over a range of cladding temperatures higher than heretofore included among the LMFBR fast-flux tests. Irradiation of this fast-flux seven-rod subassembly was started on March 2, 1971, and to date has received an exposure of approximately 7,000 MWd/Te. Irradiation of the subassembly was again interrupted because

of trouble with other EBR-II experiments, but it was reinstalled for the continuation of irradiation during Run 50E.

Fabrication of the hardware for the five F-1 replacement rods has been completed, and temperature monitors and dosimeters are being installed in the capsule thermal barriers.

Performance tests are being made on the SiC temperature monitors. Five monitors were irradiated in the ETR, and preliminary postirradiation annealing tests have been performed. Experiments are also in progress to verify another technique for monitoring fuel-rod cladding temperatures on noninstrumented irradiation capsules. This technique is based on measuring the release rates of noble fission gases from the cladding during postirradiation annealing.

Irradiation experiments F-2 and F-3 are currently being planned. The F-2 experiment is planned to be a pressurized, sealed blanket rod that will be irradiated in an EBR-II blanket row. The objectives for experiment F-3 are expected to be similar to those for the F-1, except that F-3 would be in an EBR-II core position where a higher cladding fluence can be obtained.

1.4. TASK 4700 - NUCLEAR ANALYSIS AND REACTOR PHYSICS

This task involves the evaluation of current fast reactor physics methods and data for GCFR application and the planning of a critical essembly program.

The background and objectives of the GCFR critical assembly program are discussed. The current program includes analysis of the LMFBR critical experiments being carried out at Argonne National Laboratory. Of particular interest to the GCFR program are the sodium-voided experiments in ZPPR assembly 2.

2. TASK 1000 — PROGRAM PLANNING

The formulation of a comprehensive research and development program to support the design and contruction of a GCFR demonstration plant is continuing as previously described. The results of this effort will be the publication of a document in which the development problems will be identified and defined, the tests and analytical efforts necessary for resolving them described, and costs and schedules prepared.

The first volume reviews the design of the 300-MW(e) GCFR demonstration plant and the problem areas are identified that must be resolved before the final design of the plant. In identifying all necessary development items, approximately 100 design areas are reviewed and discussed in relation to background and current technological status. Input to this volume is now 99% completed, editing is nearing completion, and the final project review is in progress. It is anticipated that final draft copies of this volume will be complete in September and ready for management review.

The second volume describes the analytical and experimental programs necessary to resolve each of the defined problem areas. Initial input is 90% completed, and initial project review has begun. It is anticipated that draft copies will be ready for management review in November.

Work on the costing and scheduling of these developmental tasks is beginning.

3. TASK 4100 — CORE DEVELOPMENT

3.1. CORE SUPPORT

An engineering analysis was made on the grid plate to determine the interactions between the grid plate and the pressure equalization system. The mechanical and thermal effects investigated included the mechanical effects caused by stress concentration resulting from the bolt holes and the vent holes, and the thermal effects caused by heat from the fission gas products within the holes.

The core is made up of fuel and blanket elements that are supported at their upper ends by firmly clamping them to the grid plate. The grid plate is designed with sufficient stiffness that the deflection of the grid plate caused by the pressure-drop forces of the reactor coolant will not be large enough to change the reactivity by more than $0.10. This design criterion leads to low stress levels, since stiffness, rather than strength, is the factor that controls the design.

The stress analysis was made using the methods given in the ASME Boiler and Pressure Vessel Code, Section III, Nuclear Vessels, Article I-9, 1968 for perforated plates. For the ideal grid plate without bolt holes or vent system holes, the maximum local stress intensity across a centrally located ligament on either the upper or lower surface is 6600 psi, which is considerable less than the primary stress allowable of 26,000 psi at the design temperature. The significant stress raisers are the bolt holes used to tie down the vent lines across the top of the grid plate, and the vent holes which penetrate the grid plate. In both cases the design margin exceeds a factor of two between stress intensity for the combined stress concentrations including thermal stresses and the combined stress allowable given by the code.

3.2. FUEL ROD ANALYSIS

The Argonne fuel lifetime code LIFE-1 has been successfully converted for the UNIVAC 1108. The principal difference between this code and BRITL appears to be the method of calculating fuel swelling. BRITL uses an empirical equation based on available data, whereas LIFE makes a direct calculation based on retained fission products. The LIFE method results in a considerably higher swelling rate.

Work is continuing in order to resolve the differences between these codes.

3.3. PRESSURE EQUALIZATION SYSTEM

The vent line connections to the fuel elements are arranged so that each element has a set of lines which are uniquely different from those to any other element so that a fuel element with a leaking rod can be specifically identified. Also, study showed not only that the existing connection pattern could be extended to include the blanket elements if required, but also that a reduction in the number of lines could be achieved by a new pattern that would interconnect sets of lines.

4. TASK 4200/4400 — FUELS AND MATERIALS DEVELOPMENT

4.1. CLADDING SURVEILLANCE

Since the design of GCFR fuel assemblies is based on LMFBR fuel technology to the maximum extent possible consistent with objectives, LMFBR-related work on fast-flux fuel irradiations, irradiation-induced metal swelling, and the mechanical properties of structural materials is closely followed. This surveillance is maintained with the short-term objective of providing the best up-to-date design data and with the longer term objective of taking timely advantage of improvements in cladding technology.

Relevant experimental results obtained at other sites in the U.S. and overseas are followed by means of USAEC and laboratory quarterly reports, topical reports, journal publications, and attendance at technical meetings. The 1971 International Conference on Radiation-Induced Voids in Metals, held at Albany, New York, June 9-11, 1971, was a very useful source of information because of the rapid progress in this field and the fact that major groups working on this problem in the U.S. and Europe were represented. Several significant developments were reported at this conference. Among new techniques for studying void formation in the laboratory, heavy-ion bombardment of thin foils followed by transmission electron microscopy, and direct observation of void formation in samples damaged in situ in the 1-MeV electron microscope have proved very productive. The saturation of total void volume at approximately 10% to 15% in very heavily ion-bombarded stainless steel and nickel samples offers the possibility of a limit to the amount of swelling that may be found under fast-reactor conditions, although saturation has not yet been confirmed for neutron-irradiated samples. The effectiveness of cold-working in reducing or suppressing void formation in materials such as Type 316 stainless steel that develop dense and very stable dislocation networks has been confirmed. Other promising metallurgical developments include observations at DFR based on nimonic PE-16

that a very fine dispersion of coherent precipitates may lead to reduced swelling, and work suggesting that stainless steels with very low carbon or stabilized with niobium or titanium additions may be swelling resistant. Among present-day conventional cladding materials, it seems that 20% cold-worked Type 316 stainless steel remains a good choice from the point of view of swelling, at least for temperatures below its recovery temperature.

4.2. THERMAL FLUX TESTS

4.2.1. Irradiation Capsule GB-9

The vented fuel rod capsule experiment GB-9 is continuing to operate satisfactorily at design power (16 kW/ft) and design cladding temperature (∿700°C) in the ORR and has achieved a burnup of about 43,000 MWd/Te to date toward the goal of 75,000 MWd/Te (Ref. 1).

Capsule GB-9 contains a charcoal trap that retains volatile fission products until the saturation level is reached, but acts only as a delay bed for the noble fission gases. During the week of May 10, 1971, tests were conducted to determine the effectiveness of the charcoal trap in delaying xenon and krypton as a function of temperature. The tests were conducted at trap temperatures of 200°, 300°, and 400°C while the capsule was held at power constant at about 16kW/ft. The capsule helium sweep gas was analyzed for fission products released from the trap and from the fuel at the various trap temperatures.

The release of gaseous fission products from the fuel remained relatively constant as would be expected, whereas the release from the trap increased by a factor of as much as eight when the trap temperature was increased from 200° to 400°C. The relative increase for the various krypton and xenon isotopes varied from less than a factor of two for Kr^{85m} up to a factor of eight for Xe^{135m} (see Figs. 4.1 and 4.2).

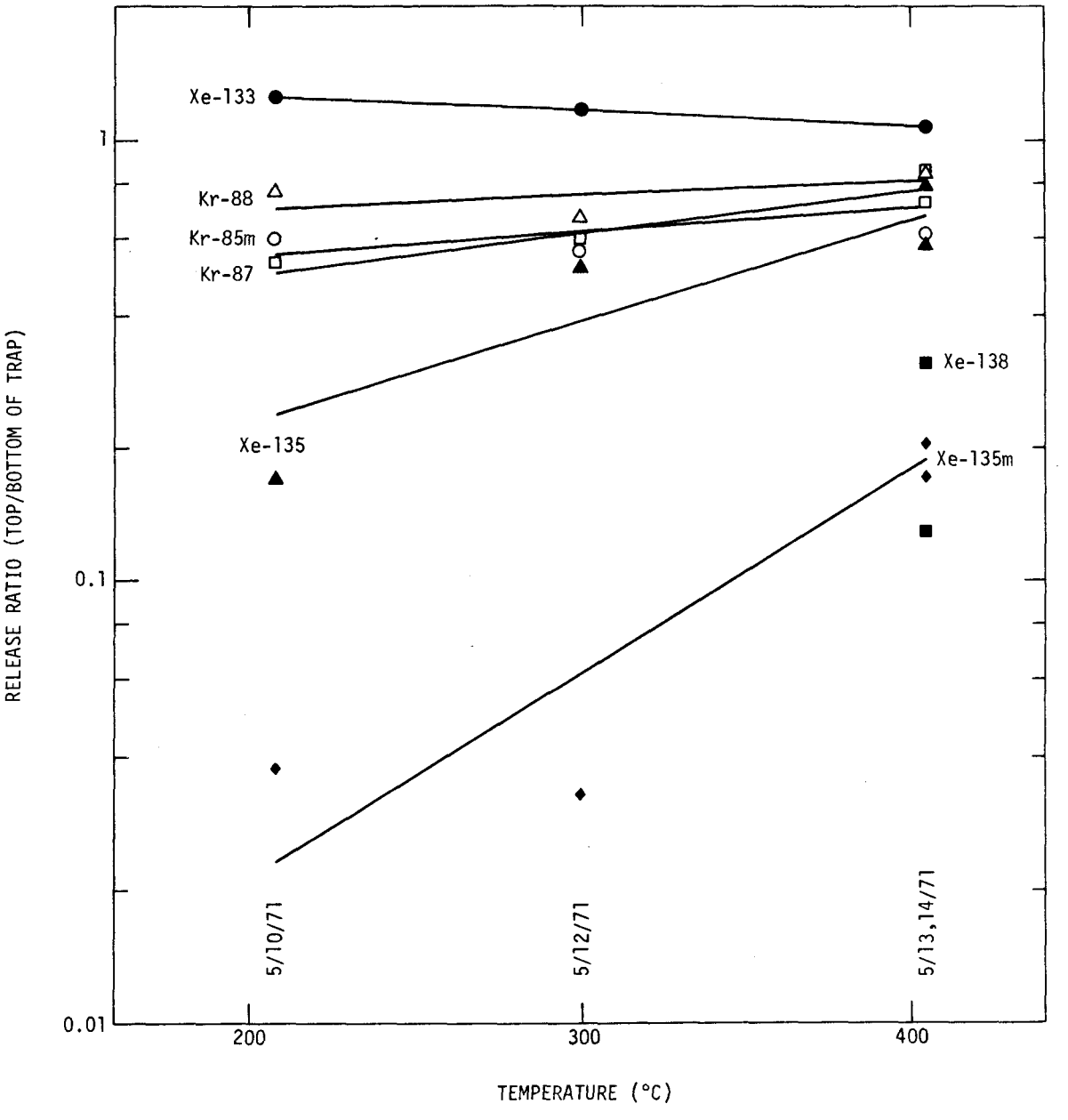

Fig. 4.1. Effectiveness of the rod trap in reducing the steady-state release from capsule GB-9. Ratio of fission gas release rate to birth rate at trap outlet to trap inlet versus trap temperature

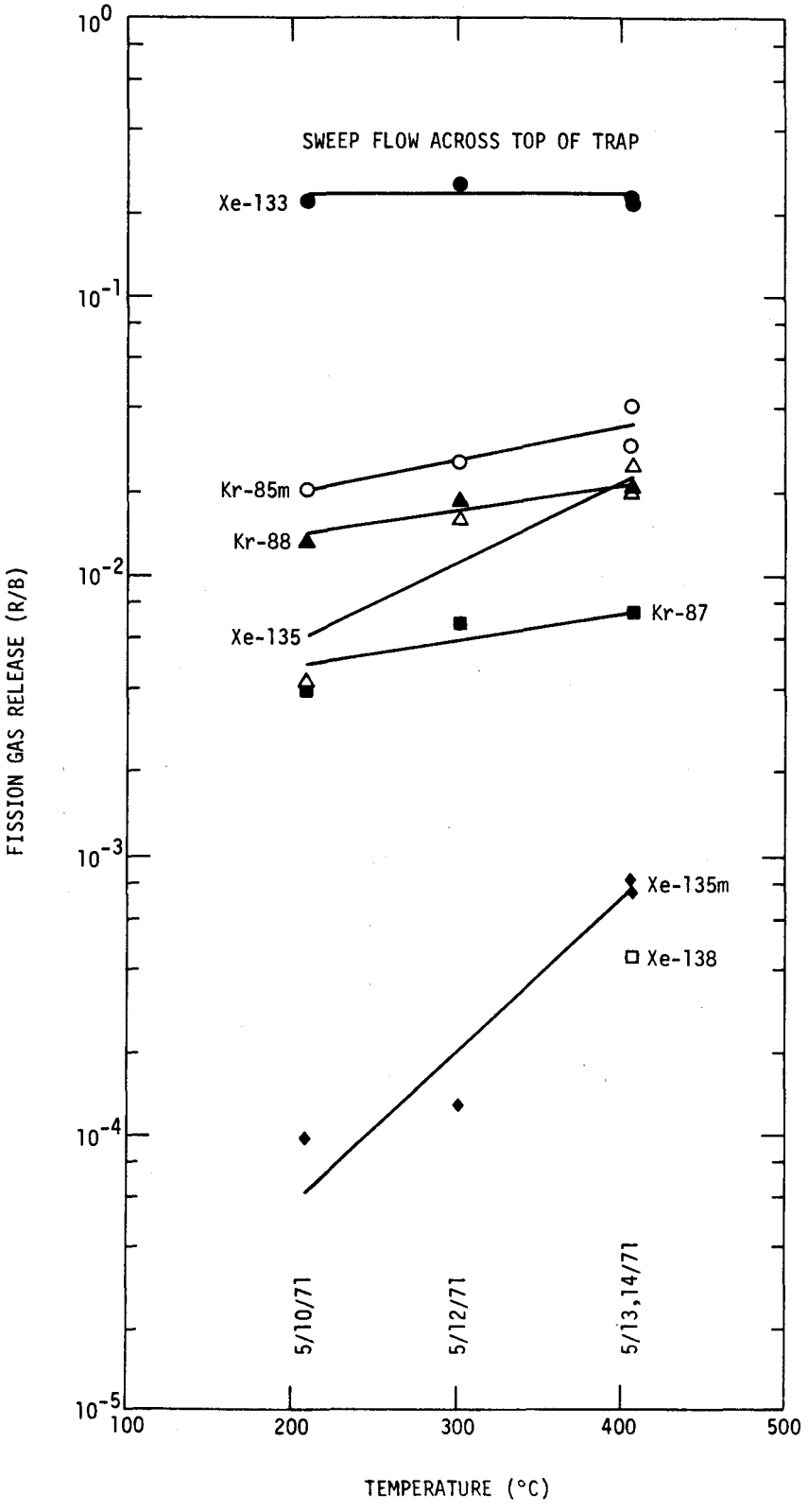

Fig. 4.2. Steady-state fission gas release from capsule GB-9 at full power versus carbon trap temperature (sweep flow across top of trap)

In addition to the trap effectiveness studies, experiments were conducted to determine the increase in fission gas release as a function of fuel rod power and cladding temperature. The helium sweep gas was analyzed for fission products released from the trap and fuel at hot-side cladding temperatures of 552°, 626°, and 682°C. The release from the fuel and trap showed a linear increase with increasing cladding temperature and maintained a constant trap-to-fuel release ratio with increasing temperature. A factor of ten increase in total fission gas release activity was observed when the cladding temperature was increased from 552° to 682°C. This is equivalent to an increase of approximately 30% in fuel rod power (see Fig. 4.3).

In order to facilitate the measurement of fission gas release from GB-9 $(Pu,U)O_2$ fuel, experiments will be performed at design power and temperature but at different pressures (i.e., 500, 750, and 1000 psi). The fission gas diffusion rate through the gas phase is inversely proportional to the helium plus fission gas pressure in the fuel rod, while the fission gas diffusion through the $(Pu,U)O_2$ fuel remains unaffected. Therefore, analysis following measurements of fission gas release at different operating pressures should allow interpretation of the fractional release from the fuel. It is also planned to perform mass spectrometer measurements of stable fission gas release from capsule GB-9 during the next quarter.

4.2.2. Irradiation Capsule GB-10

Design and analysis for vented-fuel-rod capsule GB-10 for which the objectives and design were previously reported (Ref. 2) continues. Based on heat-transfer results for surface-roughened cladding, the geometry of the roughening for the cladding for the GB-10 fuel rod has been changed from that originally specified. Consequently, new cladding tubes for the fuel rod are being fabricated. Leak checks and metallography performed on brazed (Nicrobraze 50) mockups of the gas line and thermocouple feedthroughs for the GB-10 fuel rod have shown them to be satisfactory.

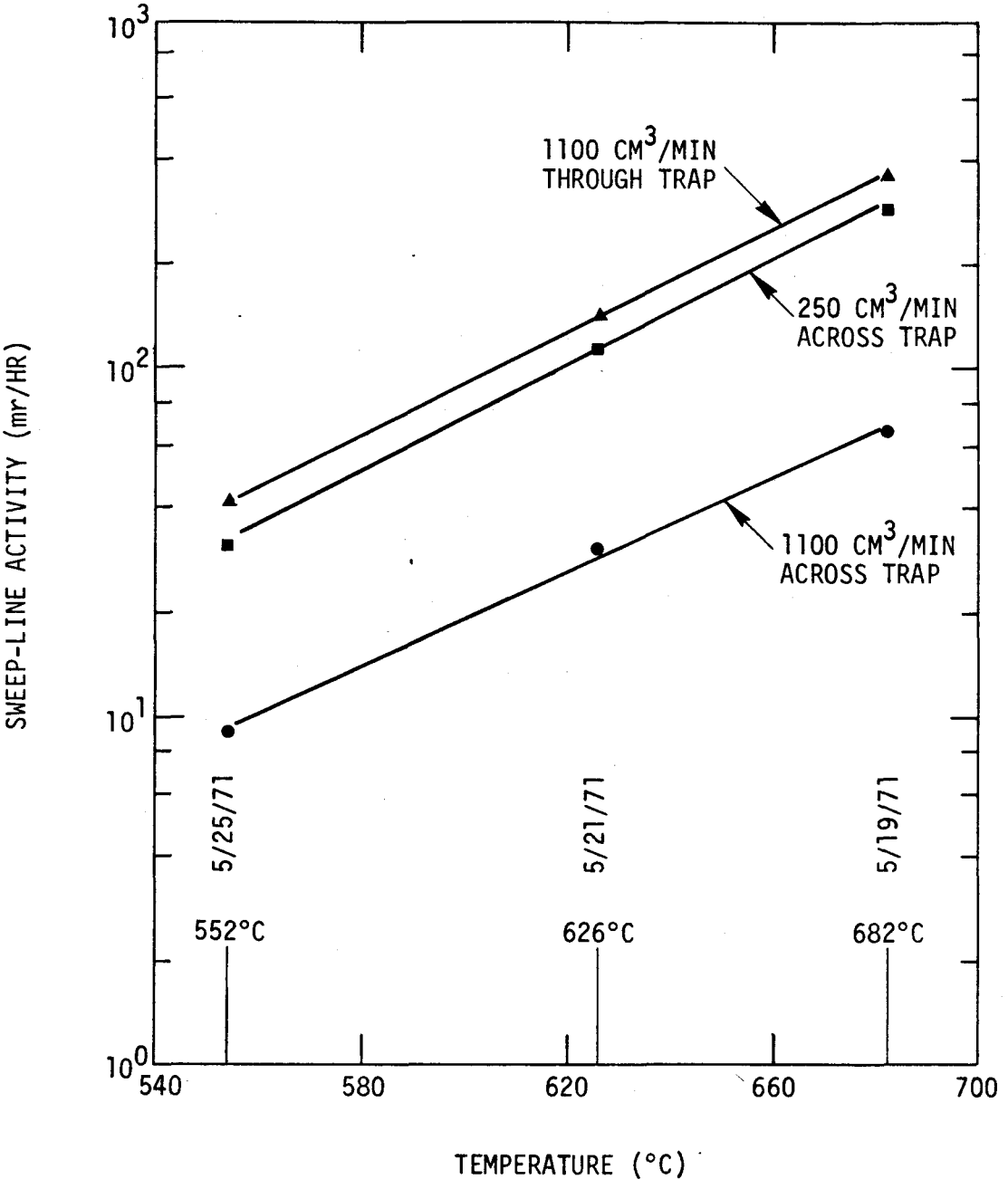

Fig. 4.3. Steady-state effluent line activity in capsule GB-9 versus calculated hot-side clad temperature

A schedule for completion of assembling the fuel rod and capsule early in 1972 has been agreed upon by Gulf General Atomic and ORNL.

Some difficulties have been experienced from time to time with the SLIDER computer code in calculating release fractions when small differences in very large numbers are required. These differences occur in order to obtain the concentration gradient across the boundary of interest from which the release rate and release fraction are computed. An alternative method has been introduced that appears to work very well. In this method, the residual concentration is integrated over various regions of interest. The release is then computed by subtracting the residual from that initially present or injected from a source.

4.3. FAST-FLUX IRRADIATION TESTS

4.3.1. Fast-Flux Irradiation Experiment F1 (X094)

The seven encapsulated fuel rods in the F1 (X094) experiment (Ref. 3) have achieved an exposure of approximately 7000 MWd/Te since startup of the EBR-II on March 2, 1971. While irradiation of the F1 (X094) experiment was again delayed by difficulties with leaking fuel rods from another experimental program in EBR-II, the experiment was reinserted for the start of EBR-II run 50F (early July) and its irradiation now is progressing.

The machining and quality assurance inspection of the hardware for the five replacement capsules (Ref. 2) for the F1 (X094) experiment has been completed. Hardware for welding setup and weld qualification has been delivered to ORNL. The remainder of the hardware will be delivered as soon as the assembly of the temperature monitors and dosimeters into the capsule thermal barriers is completed (scheduled for late August) and surface roughening by photoetching the cladding for two of the five fuel rods (three have smooth cladding) is completed (scheduled for late September).

A schedule for completing the assembly of the fuel rods and capsules by the end of calendar year 1971 has been worked out and agreed upon by Gulf General Atomic and ORNL. The fabrication at ORNL of the fuel for five replacement rods is reported to be about 50% complete.

4.3.2. Temperature Monitoring Method

Experiments have been undertaken during the past month to verify a technique for monitoring fuel rod cladding temperatures on noninstrumented fuel rod irradiation capsules such as in the F1 (X094) experiment presently being irradiated in EBR-II (Ref. 4). The technique is based upon the fact that the gaseous fission products xenon and krypton recoil into the cladding material at the irradiation temperature and are retained. During postirradiation annealing of the cladding material, the fission-gas release rate increases markedly when the annealing temperature exceeds the last temperature of irradiation. The current experiment was undertaken to determine whether this monitoring technique could be applied to the GCFR irradiation program.

Preliminary measurements were made at irradiation temperatures of 596° and 710°C on 2-in.-long specimens of stainless steel tubing loaded with about 20 g of UO_2 fuel pellets containing an enrichment of 14.9% U-235. The Type 316 stainless steel tubing (from the same material batch used in the GB-9 vented-fuel-rod capsule) is representative of the GCFR demonstration plant fuel rod cladding material. The specimens were irradiated to approximately 10^{15} fissions at the desired temperature in a graphite crucible in the TRIGA King Furnace under an inert atmosphere. The temperature of irradiation was monitored using a Chromel-Alumel thermocouple that was spot-welded directly to the exterior of the cladding material.

Upon completion of the irradiation, the cladding specimens were separated from the fuel pellets and transferred to a tube furnace, and the claddings were annealed over the temperature range of 300° to 1100°C. The temperature was increased 100° every half hour up to a maximum of about 1100°C and the fission gases were continuously purged with helium into a liquid-nitrogen-cooled charcoal trap. The trap was gamma counted at the

end of each half-hour collection period on the 4096-channel analyzer-computer system and the spectrum analyzed for the gaseous fission products Kr-85m, Kr-88, Kr-87, and Xe-135.

Plots of trap activity versus temperature show a distinct increase in fission-gas release rate when the approximate temperature of irradiation is exceeded (see Figs. 4.4 through 4.11). The slope of the curves above the irradiation temperature is different for each of the krypton isotopes. This difference is thought to be due to the nonequilibrium in the production-decay process of the fission product and the delay in diffusing before being released. The postirradiation temperature determination agrees with that measured directly to within 35°C. Irradiation exposures were also made at 800°C (see Fig. 4.12) to supplement the previous irradiations at 596° and 710°C. The 800°C irradiation was repeated at 820°C (see Fig. 4.13) because of the unusual shape of the initial 800° curve at temperatures above the 1100°C anneal. The Kr-85m curve for the 800°C run and the Kr-85m curve for the 820°C irradiation are essentially identical, indicating (1) that the steep slope above 1100°C is real and not an anomaly related to counting statistics and (2) that the experimental data are consistent and reproducible.

The slope above 1100°C is not presently understood. The annealing temperature of Type 316 stainless steel is approximately 1100°C, and the phenomenon observed may be related to recrystallization and grain growth. Additional experiments at elevated temperatures (up to 1500°C) will be undertaken shortly to better define the upper portion of the curve. The temperatures determined from the Kr-85m, Kr-88, Kr-87, and Xe-135 plots agree to within ±15°C of the observed irradiation temperature for both 800°C anneals. The annealing data from the 482°C run is currently being evaluated.

Temperature monitors made from hot-pressed silicon carbide are being included in the F1 (X094) capsules. In order to check the performance of these monitors, five monitors were irradiated in each of two instrumented capsules in the ETR by arrangement with Pacific Northwest Laboratory. These irradiations are now complete and postirradiation examination is in progress. The irradiation conditions were:

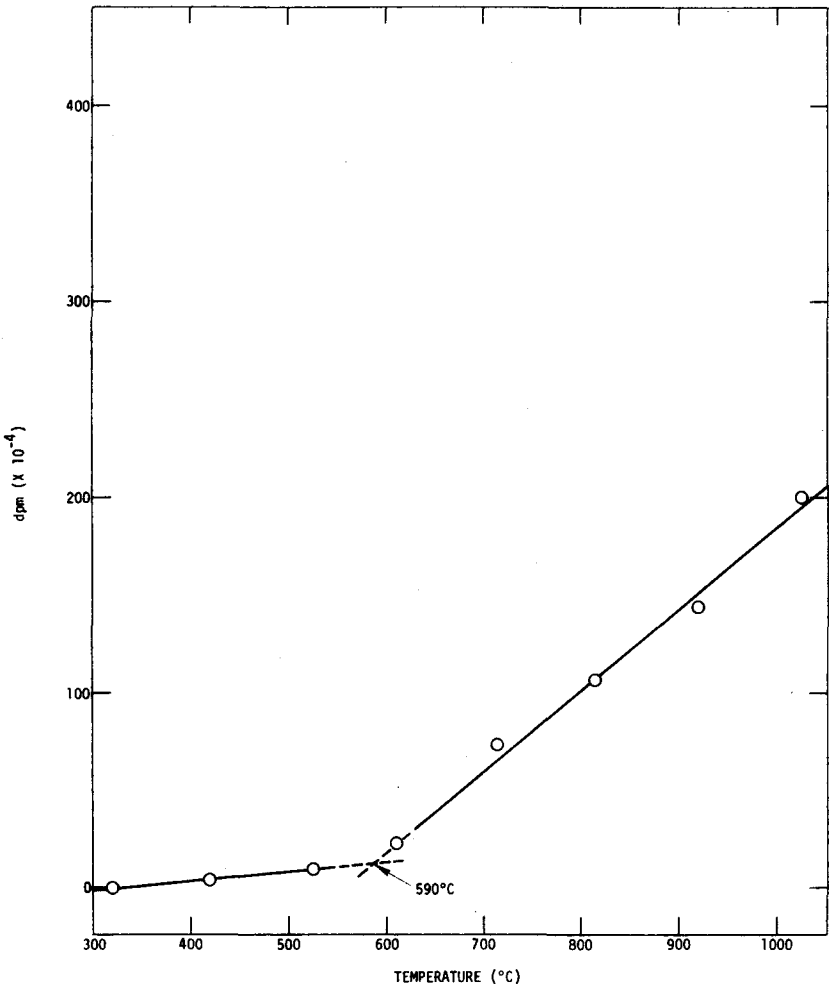

Fig. 4.4. Kr-85m release rate (irradiation temperature of 596°C)

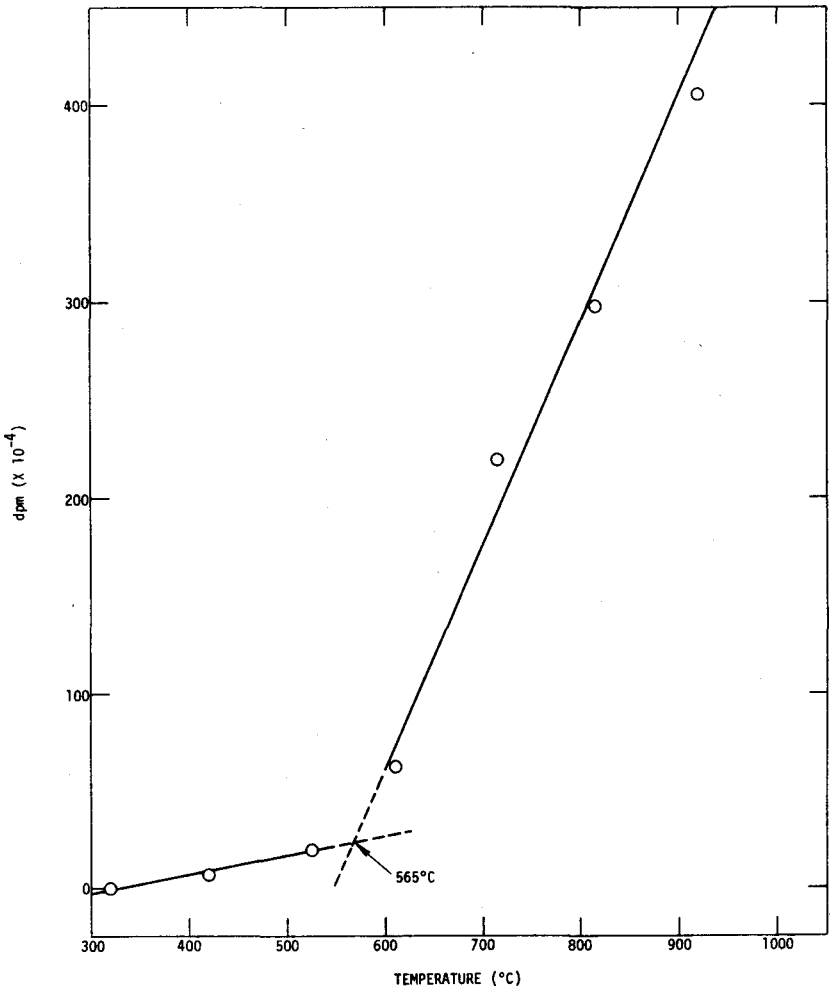

Fig. 4.5. Kr-88 release rate (irradiation temperature of 596°C)

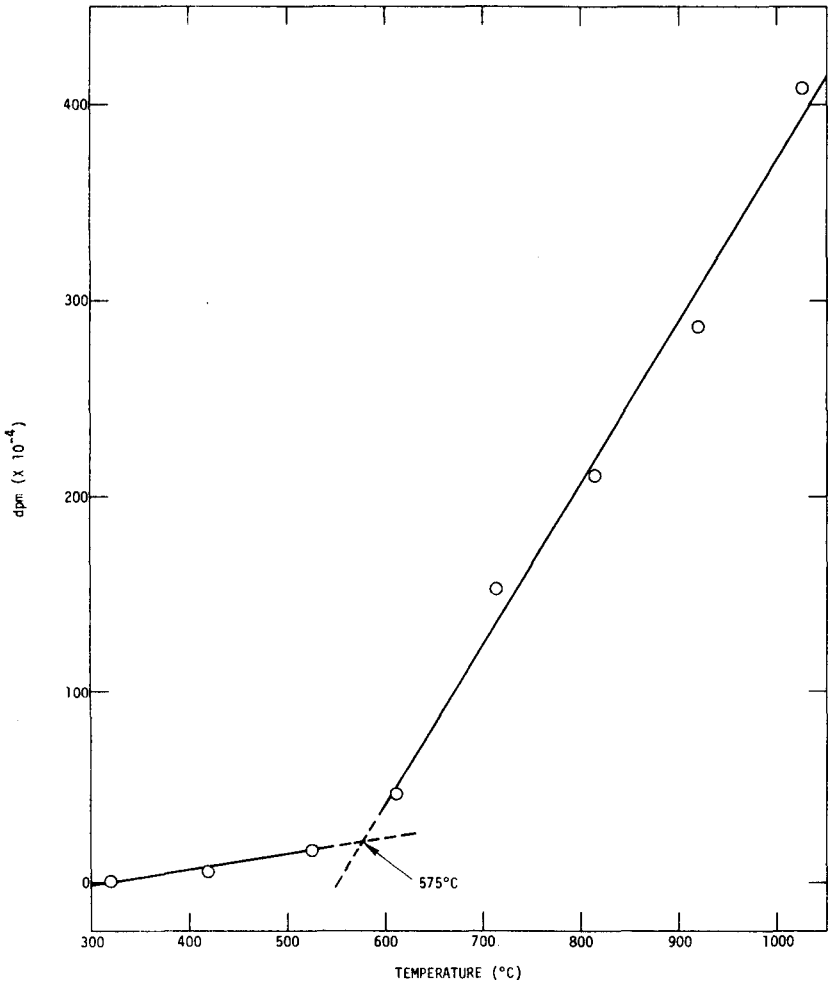

Fig. 4.6. Kr-87 release rate (irradiation temperature of 596°C)

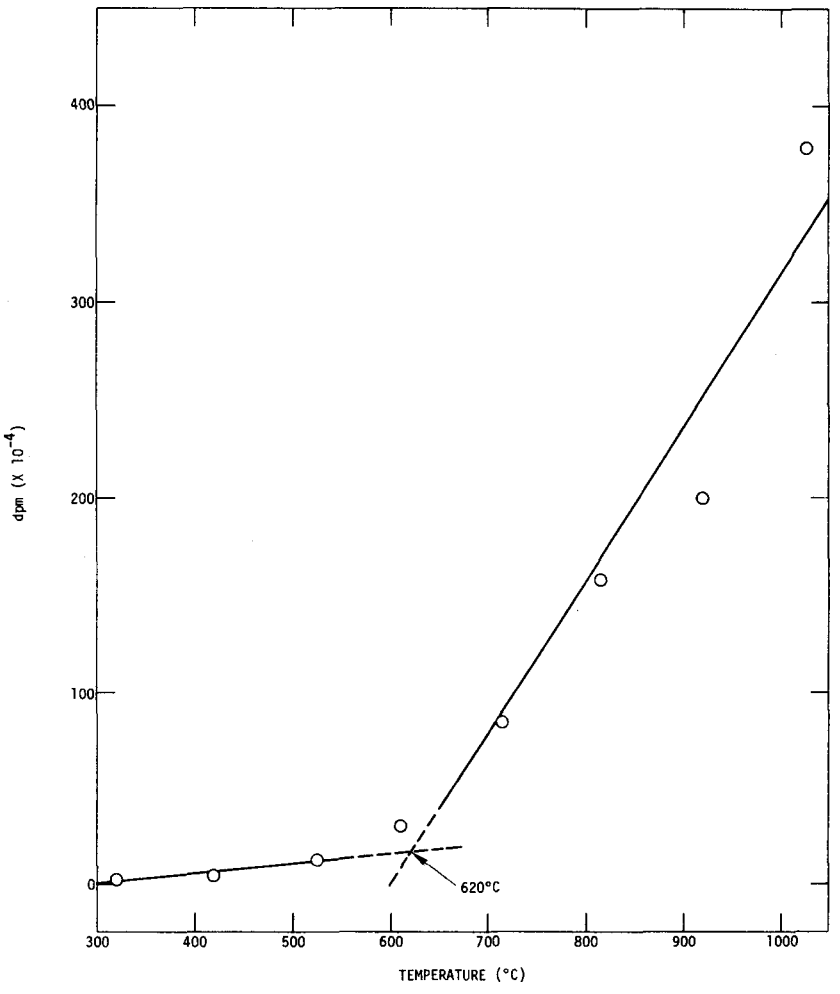

Fig. 4.7. Xe-135 release rate (irradiation temperature of 596°C)

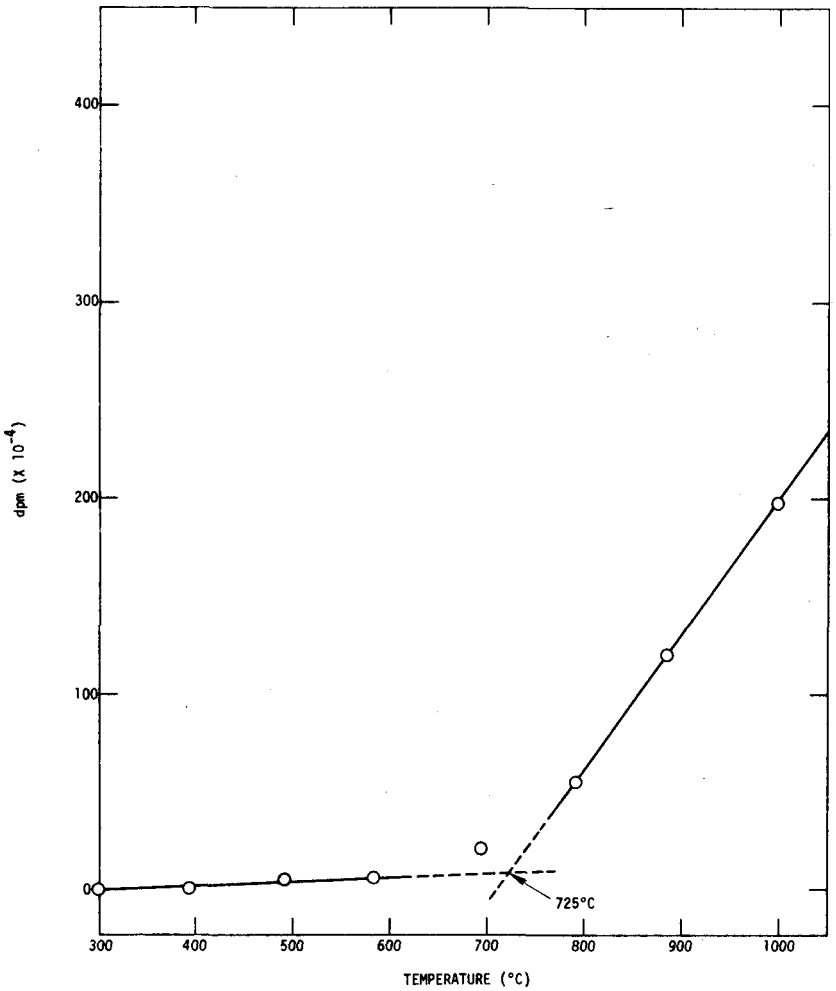

Fig. 4.8. Kr-85m release rate (irradiation temperature of 710°C)

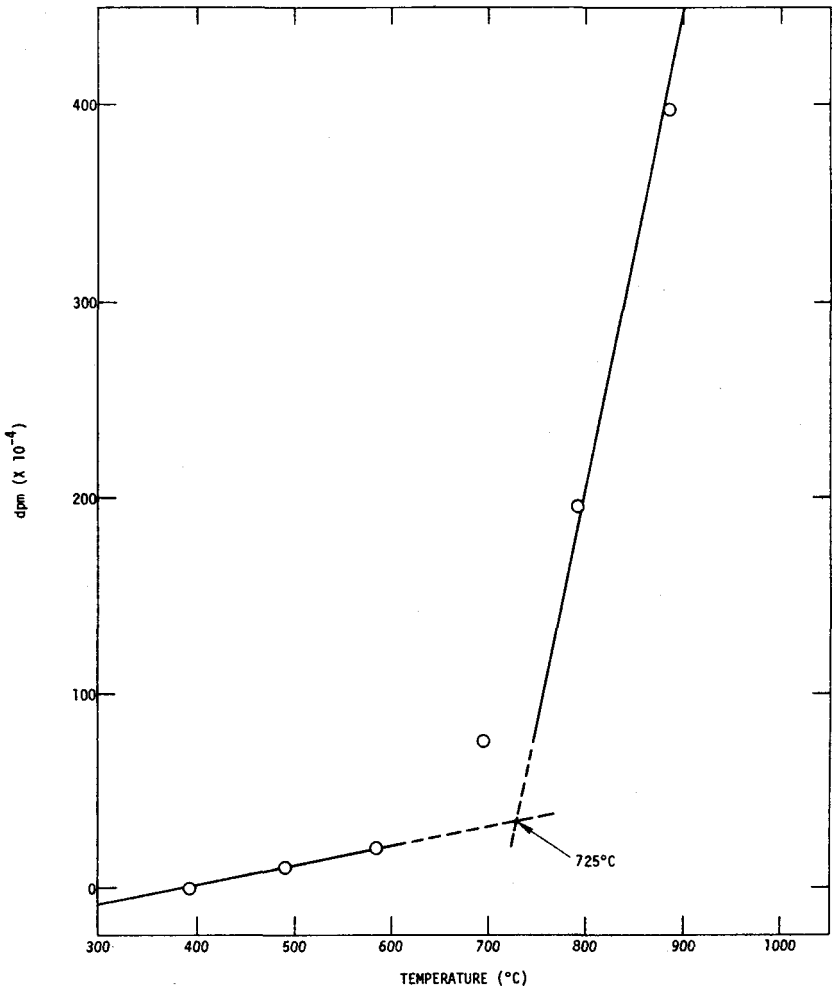

Fig. 4.9. Kr-88 release rate (irradiation temperature of 710°C)

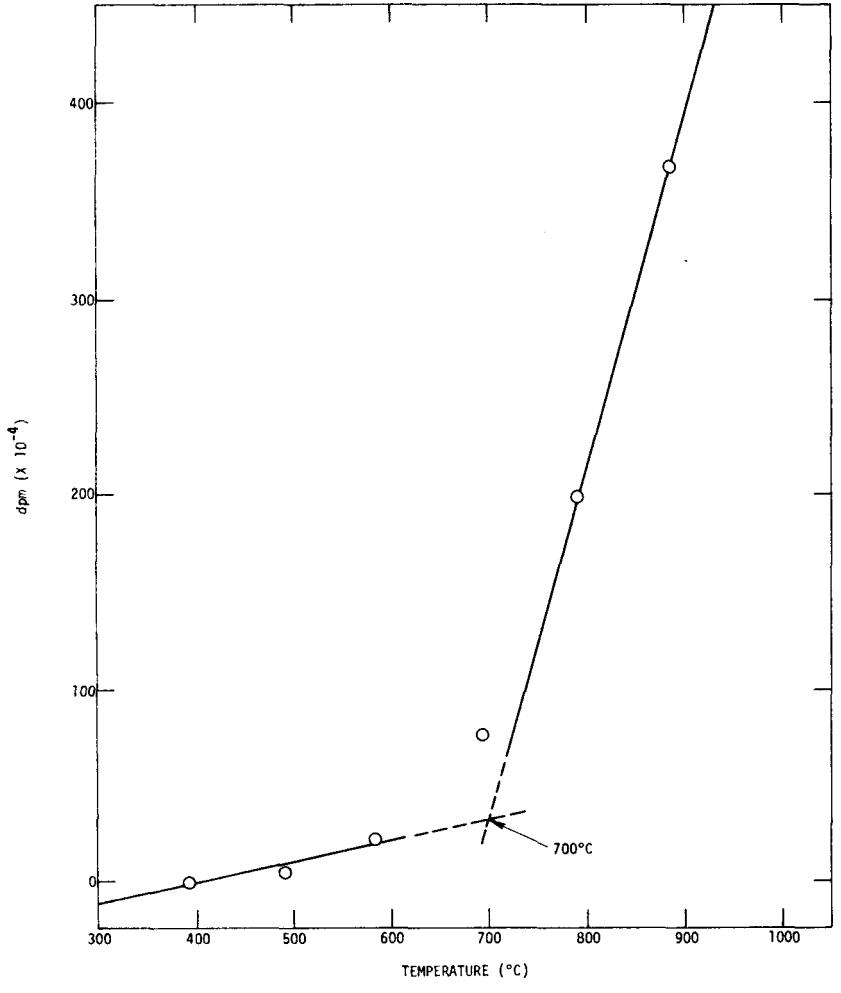

Fig. 4.10. Kr-87 release rate (irradiation temperature of 710°C)

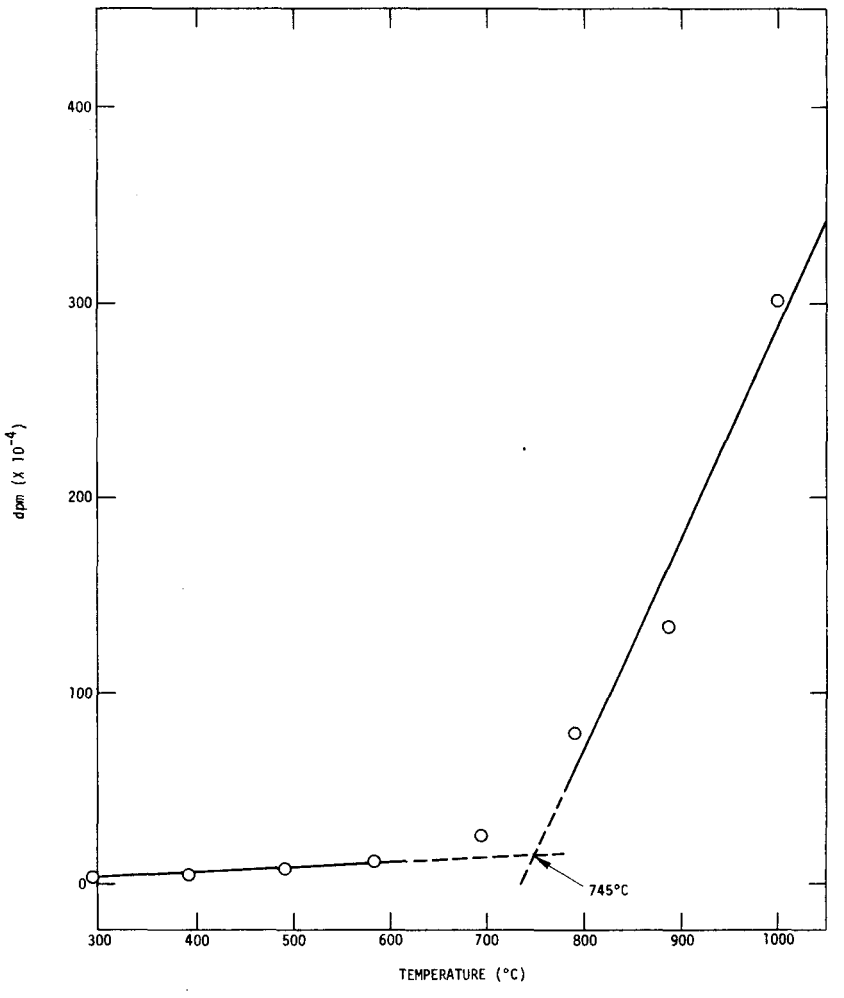

Fig. 4.11. Xe-135 release rate (irradiation temperature of 710°C)

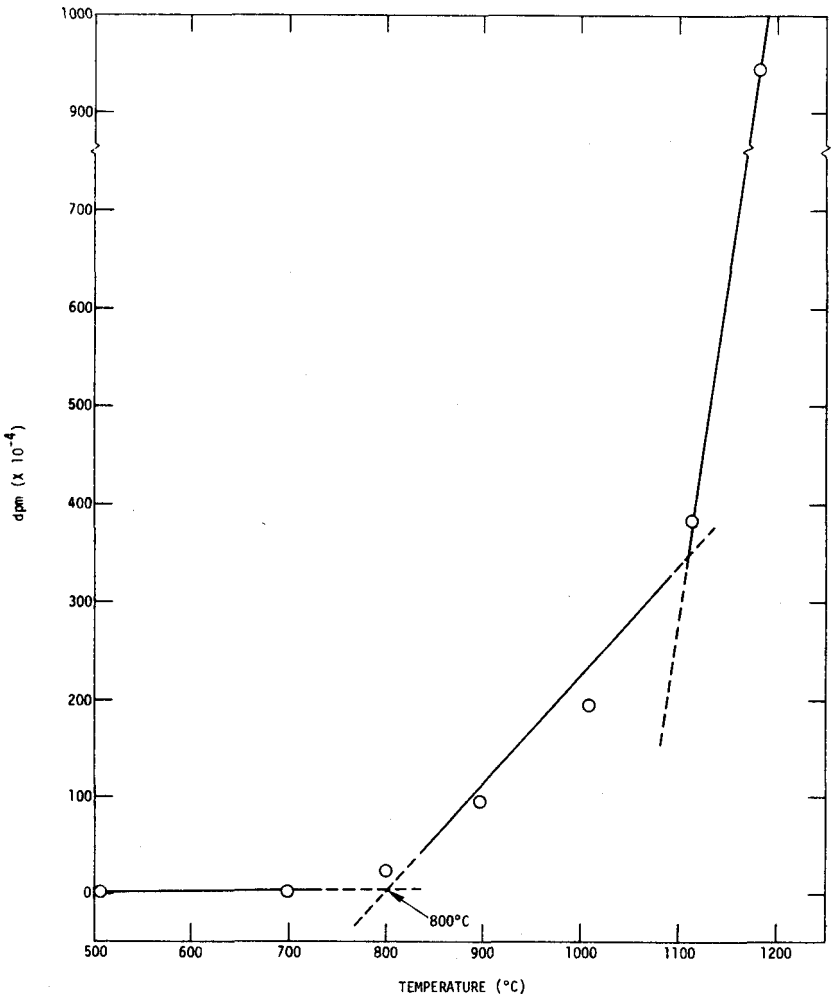

Fig. 4.12. Kr-85m release rate (irradiation temperature of 800°C)

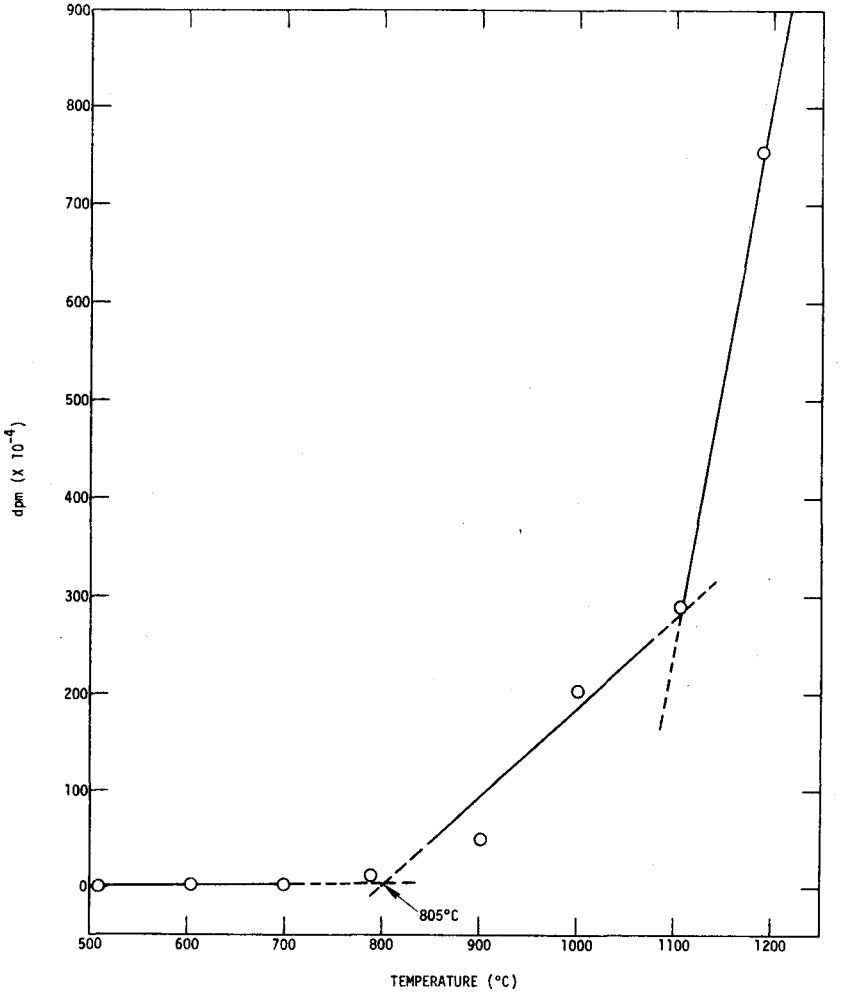

Fig. 4.13. Kr-85m release rate (irradiation temperture of 820°C)

Capsule 451:

Exposure	6.6×10^{21} n/cm^2 (E>0.18 MeV)
Mean temperature	555°C
End-of-life temperature	520°C

Capsule 481:

Exposure	6.6×10^{21} n/cm^2 (E>0.18 MeV)
Mean temperature	830°C
End-of-life temperature	777°C

Two samples from each capsule were selected for the first annealing experiment in which the samples are subjected to 1-hr anneals at temperatures increasing in increments of about 50°C, starting at 300°C. These anneals have now reached 980°C. Between each anneal, the length of each sample is measured to approximately ±25 μin. using a specially made jig, and the electrical resistivity is measured using a four-contact circuit.

As the annealing temperature reached the irradiation temperature, the dimensions of the samples started to recover toward their preirradiation dimensions. The dimensions decreased approximately linearly with increasing annealing temperature. At about the same point, the electrical resistivity of the samples started to increase exponentially with increasing annealing temperature. In one sample, the resistivity subsequently declined; in the other three the increase was monotonic. For both dimensions and resistivity the break in the annealing curves was not abrupt, but the curves tended to be sigmoidal in shape. In order to define the breakpoint, straight lines were fitted by eye to the two portions of the dimensions-versus-annealing-temperature curves and log (resistivity)-versus-annealing-temperature curves and the intersection temperature was measured. Preliminary estimates of the resulting temperatures are given in Table 4.1. There is reasonable agreement between the break temperatures and the recorded end-of-irradiation temperatures. When the annealing is completed, a least-squares procedure will be used to calculate the intersection points and the confidence limits of the estimates.

TABLE 4.1
ANNEALING CURVE BREAK POINTS OF IRRADIATED SILICON CARBIDE

Sample No.	Measured Irrad Temp (°C)		Annealing Curve Break Temp (°C)	
	Avg	Last 3 days	For Dimensions	For Resistivity
S-1	555	520	535	(430) [a]
S-2	555	520	515	510
S-5	830	777	750	720
S-6	830	777	755	750

[a] Anomalous annealing curve.

4.3.3. Fast-flux Irradiation Experiment F2

Irradiation experiment F2 as currently planned will be a pressurized, sealed 0.46-in.-diameter blanket rod experiment to be irradiated in an EBR-II blanket row position. The purpose of the experiment will be to determine the behavior of blanket rods in the presence of creep collapse of the cladding onto the blanket material and in a large flux gradient (such as occurs at the fuel - radial-blanket interface region).

A preliminary analysis was completed regarding the linear rating of a GCFR radial-blanket fuel rod in position 7N4 of the EBR-II operating at 62.5 MW(t). It was determined what the initial loading would have to be in order to achieve an 8.0 kW/ft rating after approximately 420 full power days (FPD); i.e., about two years residence at 60% load factor. Also determined were the resultant linear rating at the beginning of irradiation and the fuel composition after 420 FPD.

Results of this preliminary analysis indicate a required initial uranium enrichment of 15.6% to achieve 8.0 kW/ft at 420 FPD. This involves an initial linear rating of 8.27 kW/ft and a final fraction of Pu buildup

of 0.68% of heavy fuel metal by weight after 420 FPD. The linear rating is thus seen to stay relatively constant throughout the irradiation period. The results are summarized in Table 4.2.

TABLE 4.2
SUMMARY OF RESULTS

Parameter	Initial Values (T=0)	Final Values (T=420 FPD)
U-235 density, g/cm^3	1.356	1.236
U-238 density, g/cm^3	7.339	7.339
Pu-239 density, g/cm^3	0.0	0.0584
Linear rating, kW/ft	8.27	8.00
Enrichment, U	15.6	14.4
m_{Pu}/m_{U+Pu}	0.0	0.0068

4.3.4. Fast-flux Irradiation Experiment F3

Preliminary discussions on the objectives for experiment F3 favor objectives similar to those of the F1 (X094) experiment in progress at EBR-II, except that the experiment needs to be performed in an EBR-II core position where a higher cladding fluence can be obtained than in F1 (X094) which is being irradiated in EBR-II in the 7N4 position. Planned operating conditions will to some degree be contingent on the observations made on the examination of the first rod G-3 from the F1 (X094) experiment.

REFERENCES

1. Lindgren, J. R., et al., "Planned Thermal Irradiation of Manifolded-Vented $(U,Pu)O_2$-Fueled Rod in ERR Capsule P-9," USAEC Report GA-9896, Gulf General Atomic, March 15, 1970.

2. "Gas-Cooled Fast Breeder Reactor, Quarterly Progress Report for the Period February 1, 1971 through April 30, 1971," USAEC Report GA-10645, Gulf General Atomic, May 28, 1971.

3. Flynn, P.W., et al., "High-Temperature Fast-Flux Irradiation Experiment for Mixed-Oxide Fuel Rods," USAEC Report GA-10264, Gulf General Atomic, October 15, 1970.

4. Bramman, J. I., et al., "Temperature Measurements in Uninstrumented DFR Experiments," International Conference on Fast Reactor Irradiation Testing, Thurso, England, April 14-17, 1969, Paper No. 7/7.

5. TASK 4700 — NUCLEAR ANALYSIS AND REACTOR PHYSICS

This task is concerned at present with the surveillance of LMFBR critical experiments, with the object of providing an experimental basis for GCFR reactor physics by making use, initially, of critical assembly work done in support of the LMFBR program. As a further part of this effort, critical experiments specifically oriented to the GCFR program will be planned.

Work to date has advanced well into the calculational stages. Initially, the effort was devoted to surveying the numerous critical assemblies built and measured for the LMFBR program and to selecting the most appropriate of these for GCFR study. Of special interest were those assemblies in which the neutronic characteristics of large sodium voided regions were examined. ZPPR Assembly 2 was selected as the first assembly to be studied since it satisfied these requirements.

5.1. ZPPR ASSEMBLY 2

ZPPR Assembly 2 is a two-zoned clean assembly with composition and dimensions representative of demonstration plants. A series of experiments was done in this assembly in a sodium-voided configuration (the voided zone in the inner core is 24 in. high and has a radius of 10.88 in.) which included measurements of the neutron spectrum, reaction rates, fission ratios, Doppler coefficient, small sample reactivity, and radial traverses. These later experiments are of special value for GCFR since in a sodium-voided configuration the composition and neutron spectrum are similar to that of a GCFR in the central region. Figure 5.1 compares a 10-group spectrum in a large voided region of the inner core of ZPPR-2 with the spectra in two different locations in a GCFR demonstration plant. The spectrum in the sodium-voided region becomes asymptotic about 15 cm from

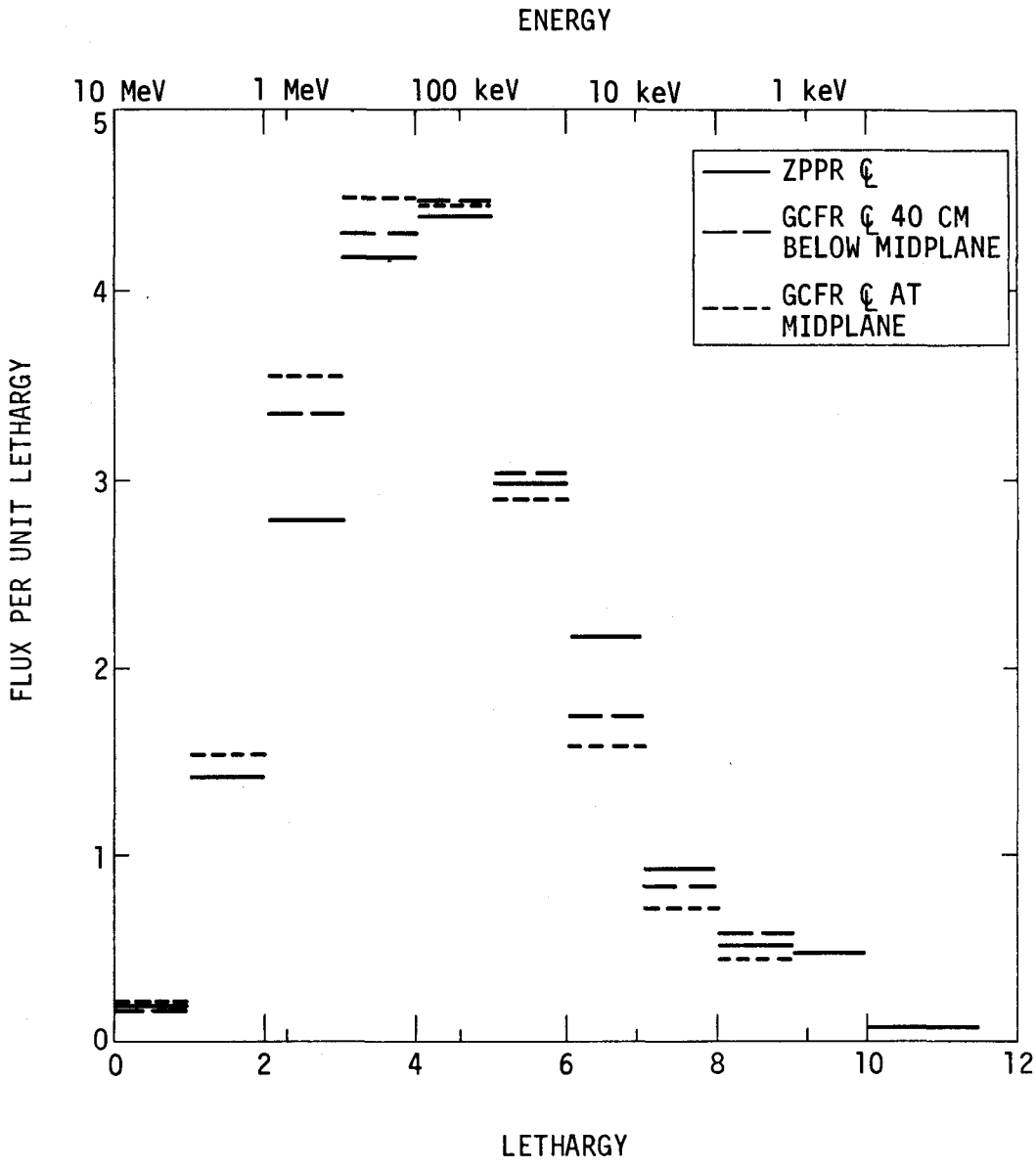

Fig. 5.1. Neutron flux as a function of lethargy for voided ZPPR-2

the edge of the region. This can be seen in Fig. 5.2 which shows part of the 27-group spectra at different space points obtained with the one-dimensional diffusion code GAZE by calculating an equivalent sphericalized ZPPR-2 reactor with a 10-in. radius center region devoid of sodium.

The average volume fractions of the core components for the GCFR demonstration plant are compared in Table 5.1 to the average volume fractions for ZPPR-2.

TABLE 5.1
AVERAGE VOLUME FRACTIONS OF GROSS COMPONENTS

	Volume Fraction (%)	
Material	ZPPR-2	GCFR
Fuel	33	30.2
Steel	20	25.2
Sodium	41	--
Void	6	44.6

Once having established the gross similarity of the ZPPR-2 spectrum and composition to GCFR, a series of more detailed calculations was planned. The first step was to establish familiarity with the special calculational procedures required for this highly heterogeneous critical assembly. Initial effort concerned neutron spectra and critical mass prediction for the case of the assembly, i.e., before sodium voiding.

5.2. SPECTRUM AND CRITICAL MASS

The GGC-5 cross section averaging code was used to determine a 99 fine group spectrum using a homogeneous model with atom densities of the inner core. This spectrum is shown in Fig. 5.3 together with the experimentally determined spectrum. Agreement is fair over most of the range except in the region above 2 MeV where the calculated values considerably exceed measured values. Other points of disagreement lie around the iron and sodium resonances

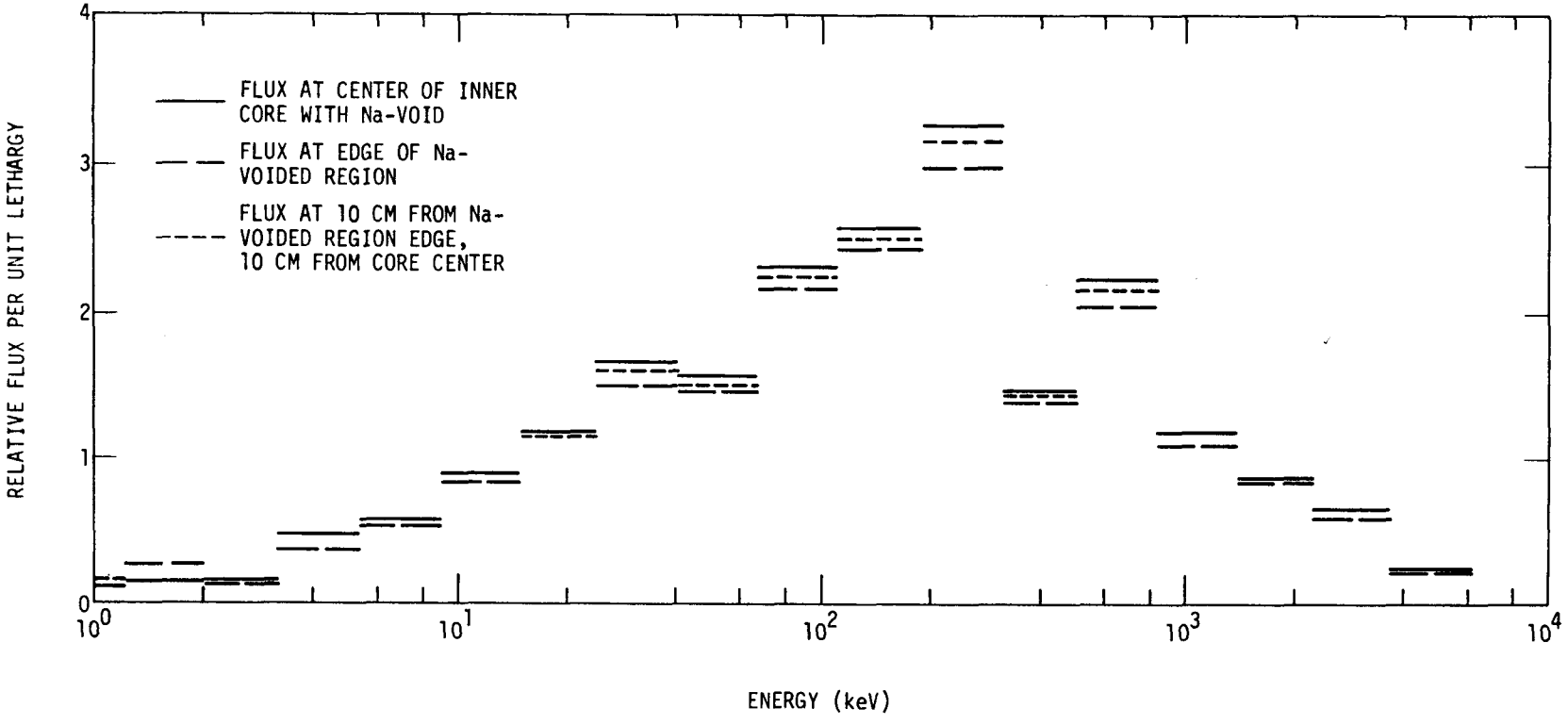

Fig. 5.2. Flux spectra in ZPPR-2 (fluxes normalized to total area)

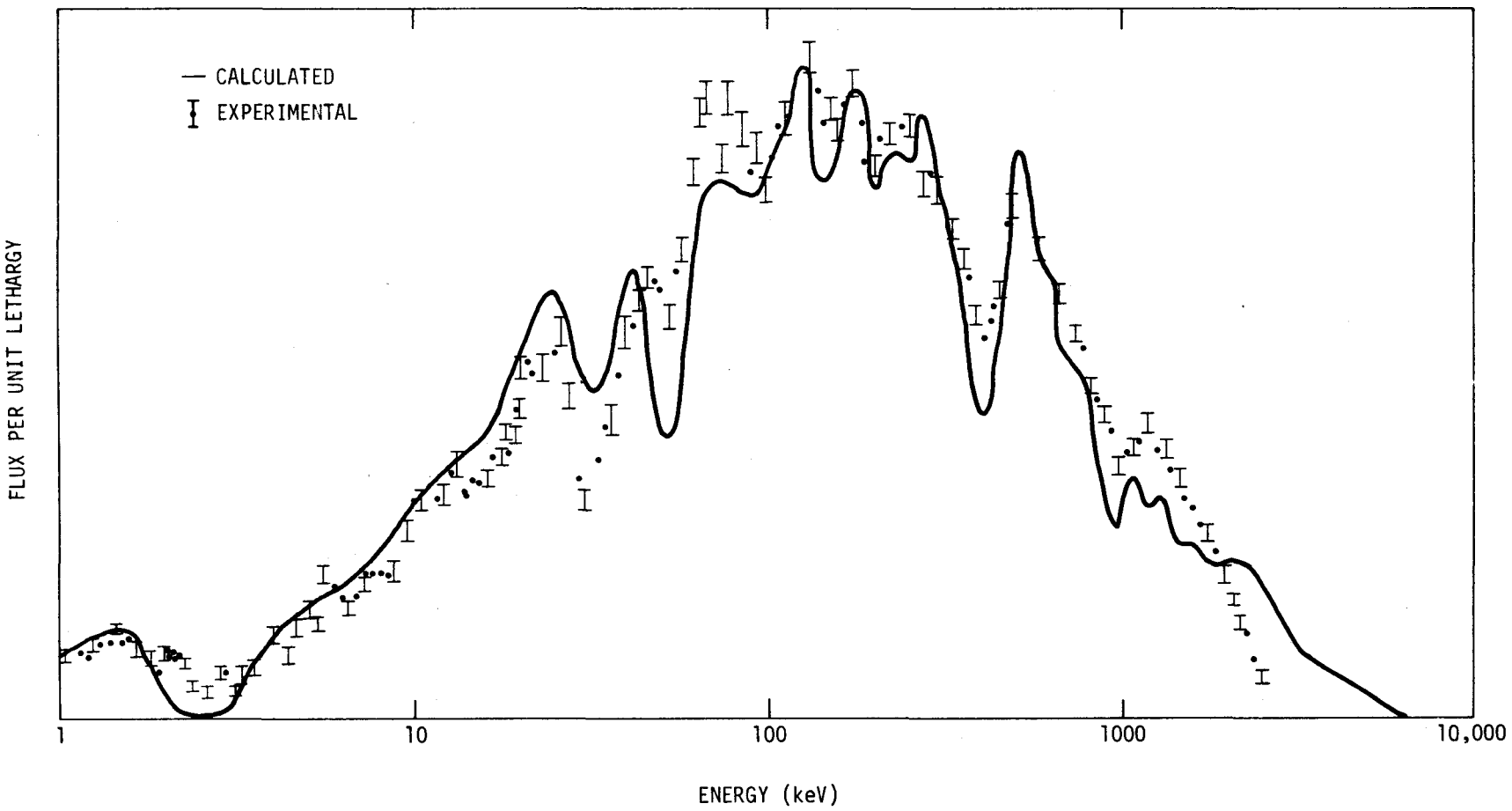

Fig. 5.3. Flux spectrum obtained with GGC-5 cross section averaging code together with experimentally determined spectrum

at 30 and 50 keV and the oxygen resonance at 400 keV. The causes of these discrepancies are being studied further.

The fine group spectrum was used to average cross sections in 27, 10, 4, and 1 energy groups with energy self shielding accounted for by using the GAROL-GANDY options of the GGC-5 code.

The critical mass calculations then proceeded in the following way:

1. Spatial self-shielding factors were determined for both inner and outer core regions using 1DF, a one-dimensional transport theory code.

2. The one-dimensional diffusion theory code, GAZE, was used in a series of axial-radial iterations to find k_{eff} of the assembly. The 27 group cross section set discussed earlier was used together with the self-shielding factors produced by the 1DF runs. The series converged quickly with the first round yielding a k_{eff} of 0.9936 and the second round, a k_{eff} of 1.0005.

The critical mass of Pu-239 + 241 in the ZPPR Assembly 2 is 984.15 kg. The reactor is, as is usual for critical assemblies, slightly subcritical at this loading. When adjusted to $k_{eff} = 1$, the corrected critical mass is 1024.3 ± 1.3 kg. The measured relationship between loading changes and k_{eff} changes is given by ANL as $\Delta M = 11.3\ (\Delta k/k)M$. On this basis the as-built k_{eff} is 0.9964. Hence the calculations for k_{eff} are within 1/2% of the experimental values. Critical mass, as may be observed from Table 5.2 differs more, but as may be deduced from the formula stated previously, such a variation is expected since the formula deals with edge worth fuel rather than homogeneous fuel addition.

TABLE 5.2
COMPARISON OF CRITICAL MASS VALUES

k_{eff}	Critical Mass (kg)	Argonne quoted mass (kg)	Δ Mass	
			(kg)	(%)
0.99364	1055.3	1024.3±1.3	+31	+3.1
1.00053	978.3		-46	-4.7

5.3. RADIAL TRAVERSES AND REACTOR RATE RATIOS

Experimental results for ZPPR-2 included radial fission rate traverses using U-238, Pu-239, and U-235. Calculations were performed to compare with these results using the following approach: The 27-group cross section set was used in a radial GAZE calculation. The energy dependent flux for every mesh point (4-cm radial spacing) was determined and used to integrate the relevant cross sections over the energy. The integral reaction rate was normalized to 1 at the centerline of the reactor.

The results can be seen in Figs. 5.4, 5.5, and 5.6 for U-238, Pu-239, and U-235, respectively. For U-238 there is disagreement at the interface region between the inner and outer core. For U-235 and Pu-239, agreement throughout the core is excellent. Some disagreement may be observed, however, in the blanket and reflector where the spectrum differs considerably from the spectrum used to average the cross section. Further attention is being given to this problem.

Table 5.3 summarizes the reaction rate ratio calculations. Fission rate ratios relative to U-235 and Pu-239 were calculated with diffusion theory for U-238, Pu-239, and Pu-240 in both the inner and outer core. Values obtained were compared to experimental values and to calculations performed at ANL.[2] ANL used both diffusion and Monte Carlo techniques.

Diffusion theory calculations of fission rate ratios relative to U-235, both by GGA and ANL, consistently underpredict experimental values. Monte

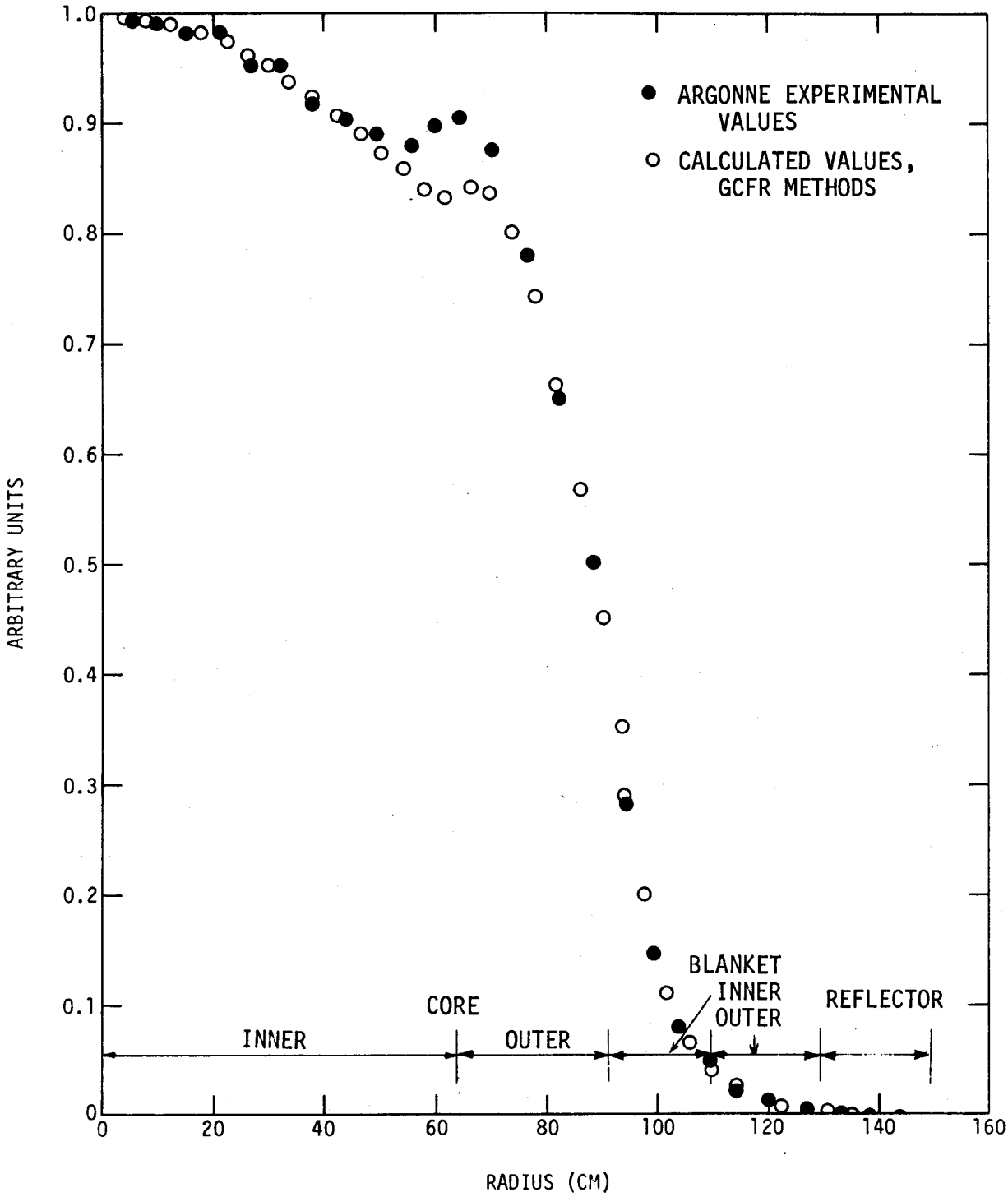

Fig. 5.4. U-238 fission rate traverse

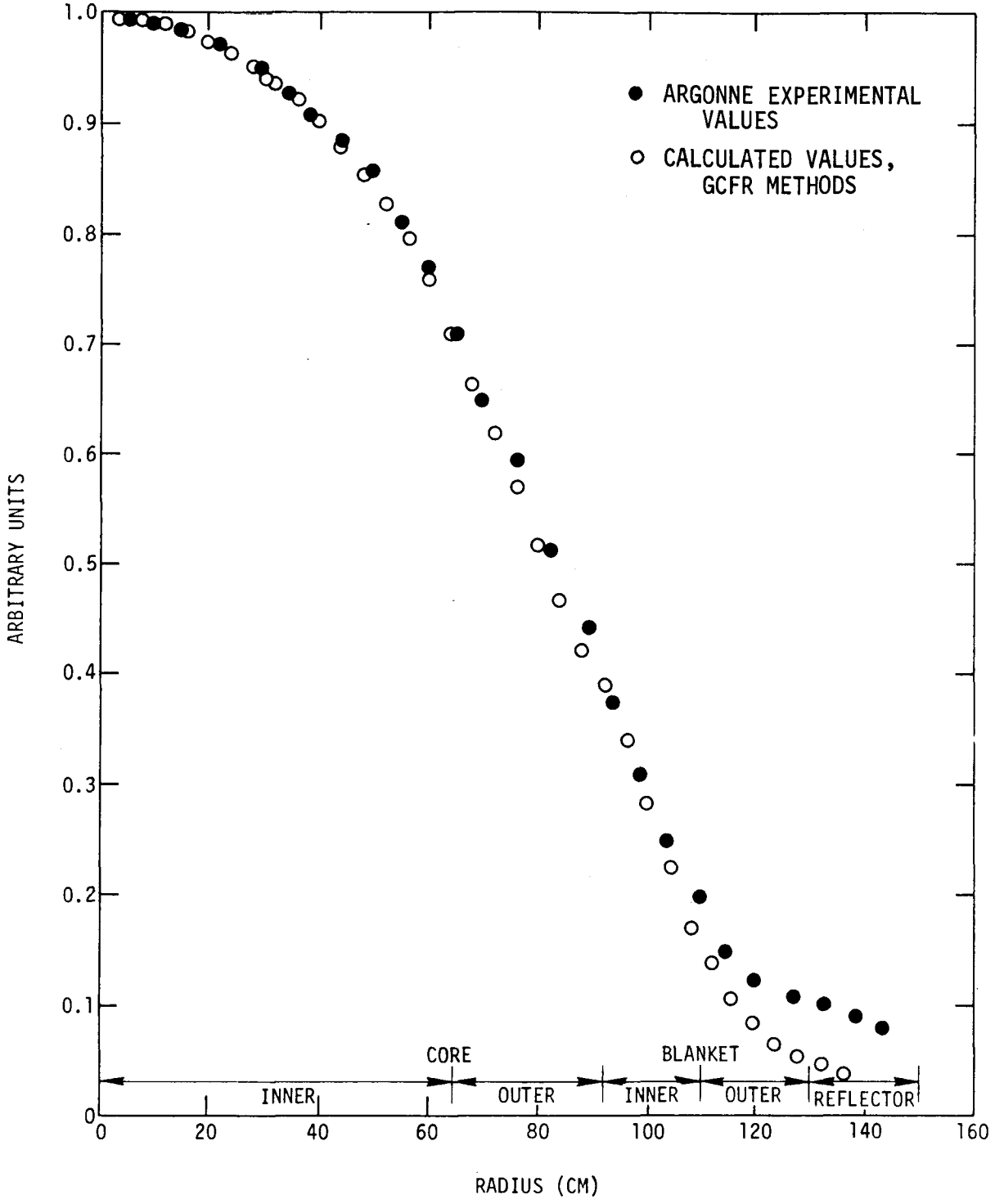

Fig. 5.5. Pu-239 fission rate traverse

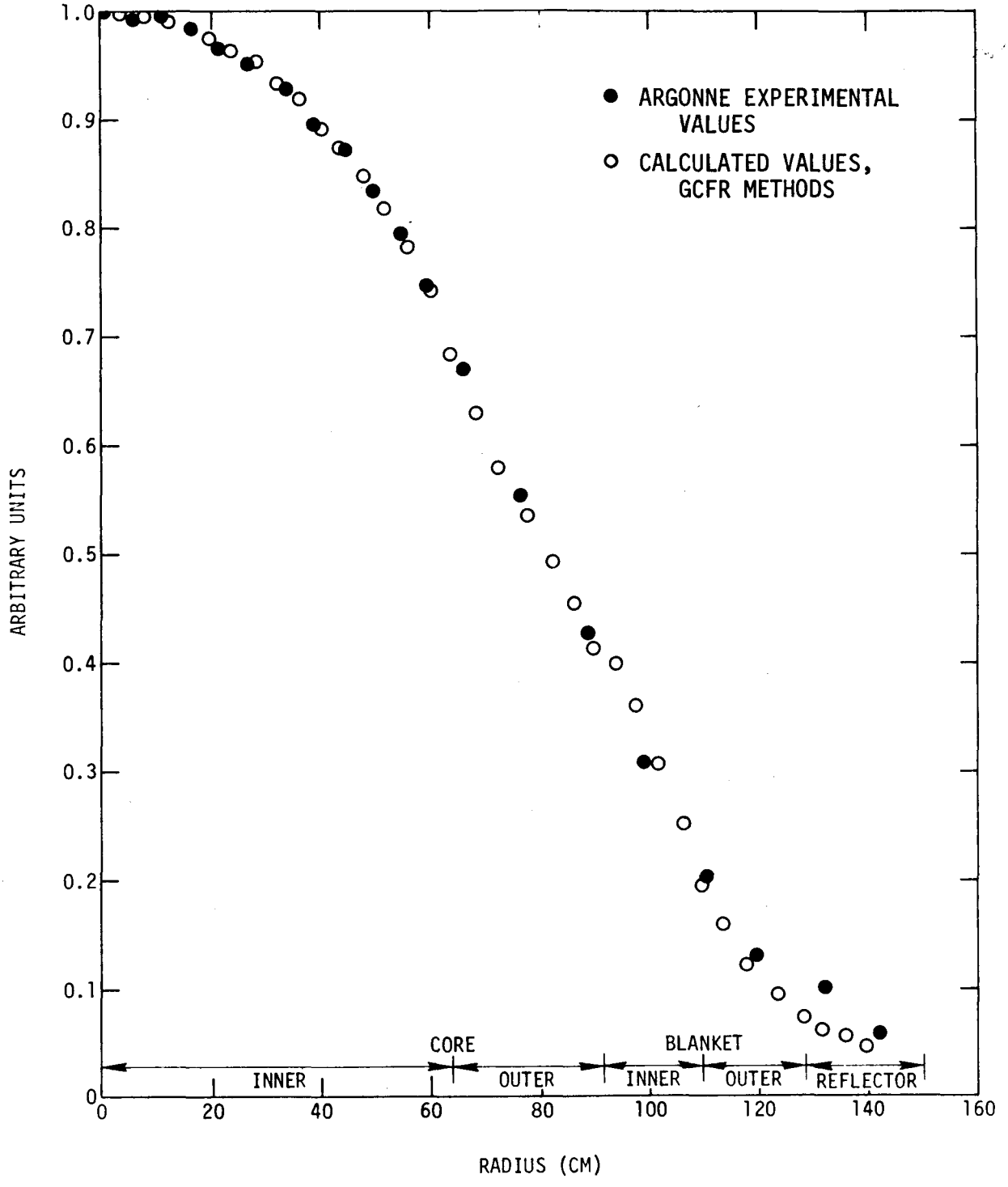

Fig. 5.6. U-235 fission rate traverse

TABLE 5.3
SUMMARY OF FISSION RATIOS FOR U-235 AND Pu-239
AND RATIO OF CAPTURE IN U-238 TO FISSION IN U-235 AND Pu-239

Isotope	Inner Core				Outer Core		
	Experimental	Calc. GGA	Calc. ANL (Diffusion) (Ref. 1)	Calc. ANL (Monte Carlo) (Ref. 2)	Experimental	Calc. GGA	Calc. ANL (Diffusion)
Fission Ratios Relative to U-235							
U-238	0.0201 ± 0.0004	0.0168	0.01866	0.0222	0.0281	0.0233	0.02564
Pu-239	0.9372 ± 0.0142	0.8360	0.8616	0.9125	0.9913	0.8833	0.9069
Pu-240	0.1704 ± 0.0026	0.1446	0.1584	0.1816	---	---	---
Fission Ratios Relative to Pu-239							
U-235	1.067 ± 0.014	1.1962	1.161	---	1.009	1.132	1.103
U-238	0.0215 ± 0.0005	0.2010	0.2166	---	0.0283	0.0264	0.02827
Pu-240	0.1818 ± 0.0047	0.1730	0.1839	---	---	---	---

Ratio of Capture in U-238 to Fission in U-235 and Pu-239[(a)]

	Inner Core		Outer Core	
	Calc. ANL	Calc. GGA	Calc. ANL	Calc. GGA
U-238(n,γ)/Pu-239(n,f)	0.1637	0.1590	0.1553	0.1504
U-238(n,γ)/U-235(n,f)	0.1411	0.1329	0.1409	0.1329

Carlo calculations are much closer to the experiment and, in general, overpredict the fission ratios slightly. This may indicate that the problem is more in the analytical modeling of the detector than in the cross sections or the spectra.

GGA diffusion calculations appear to underpredict fission ratios even more than do the ANL calculations. GGA underpredicts experiment for U-235 ratios by 12-16% while ANL underpredicts by only 7-9%. ANL predicts ratios relative to Pu-239 fission quite well while GGA results underpredict by 4-7%. Further work is planned to resolve these discrepancies.

For the ratio of capture in U-238 to the fission in U-235 and Pu-239, there are no experimental data but there are calculations by ANL. GGA calculations predict lower ratios by 2.5% relative to Pu-239 and 6% relative to U-235 than does ANL.

5.4. TWO-DIMENSIONAL CRITICALITY CALCULATIONS AND GROUP-COLLAPSING TECHNIQUE

A two-dimensional criticality calculation for ZPPR-2 is presently under way. The following technique is being used:

1. Generate 27-group cross sections for the homogeneous inner core of ZPPR-2 using the GGC-5 code.

2. Correct the cross sections with spatial self-shielding factors which are calculated by the 1DF code.

3. Using the one-dimensional diffusion code, GAZE, obtain 27-group fluxes in several regions of ZPPR-2.

4. Collapse the 27-group cross sections to 4 groups in as many regions of the reactor as required to account for the spatial variation of the spectrum.

5. Using the 4-group collapsed cross sections, generate macroscopic cross sections for each region. This is done in order to simplify data handling.

6. Finally, use these macroscopic cross sections in BUG2, a two-dimensional diffusion code to calculate k_{eff}.

To show the validity of the collapsing procedure, a test case was run, in which a spherical equivalent to the ZPPR-2 reactor was calculated by the GAZE code using the original 27-group cross sections, and subsequently the 4-group and 1-group collapsed cross sections. The results are summarized in Table 5.4.

TABLE 5.4
RESULTS OF TEST CASE USING THE GAZE CODE

Groups	k_{eff}
27	1.01025
4	1.00950
1	1.01018

REFERENCES

1. ZPR, Technical Memoranda Nos. 41, 48, 51.
2. "Reactor Development Program Progress Report, February 1971," Argonne National Laboratory Report ANL-7783, March 22, 1971.

APPENDIX

PUBLICATIONS

"Fuel Element Development for Gas-Cooled Fast Breeder Reactor (GCFR). Part 2. Vented Fuel-rod Development," by R. J. Camipana, J. R. Lindgren, and N. L. Baldwin (GGA) and A. W. Longest, Jr. (ORNL), paper presented at the ANS Annual Meeting, Boston, Mass., June 13-17, 1971 (GA-10657, June 8, 1971).